



Application of a Unified Land Model for Estimation of the Terrestrial Water Balance



Ben Livneh¹, Dennis. P. Lettenmaier¹, Pedro Restrepo².

1) University of Washington Department of Civil and Environmental Engineering Box 352700, Seattle, WA 98195 (blivneh@hydro.washington.edu).
2) NOAA National Weather Service Office of Hydrologic Development, Silver Spring, MD 20910-

ABSTRACT

Approximately 60 – 80 % of precipitation is returned to the atmosphere through evapotranspiration (ET) on global average, making it a key component of the surface water budget. In-situ measurements of ET are sparse and cannot be readily interpolated over large areas given heterogeneity in land cover. Furthermore, in situ ET measurements can be subject to large measurement errors. Here, we seek to evaluate a Unified Land Model, ULM, which is a merger of the Noah land surface scheme used in NOAA's weather prediction and climate models with the Sacramento Soil Moisture Accounting Model, used by the National Weather Service for operational streamflow prediction. Our goal is to estimate regional-scale water balances, and to compare the estimates with independent ET and streamflow observations over a set of large continental U.S. river basin and their interior sub-basins. This work is motivated by two objectives, first to quantify the evaporative component of the terrestrial water balance, and second to evaluate the large-scale prediction skill of ULM. The experiments consist of comparing ET estimates from: (i) an atmospheric water balance, (ii) satellite based estimates of ET, and (iii) ULM, forced with the same precipitation data used in the atmospheric water balance.

Model description

The modeling component of this study is focused on Unified Land Model (ULM; Livneh et al., 2010). Figure 1 highlights the components that were preserved from the two parent models (Noah and Sac). The key aspects of the merger were: (i) introducing the Noah vegetation scheme into the Sac model structure, hence allowing for physically-based moisture extraction and interception as well as a dynamic potential evapotranspiration (PET) estimation; and (ii) converting Sac's conceptual moisture storages into physical layers for computation of heat exchange, via an adaptation of the method of Koren et al. (2008).

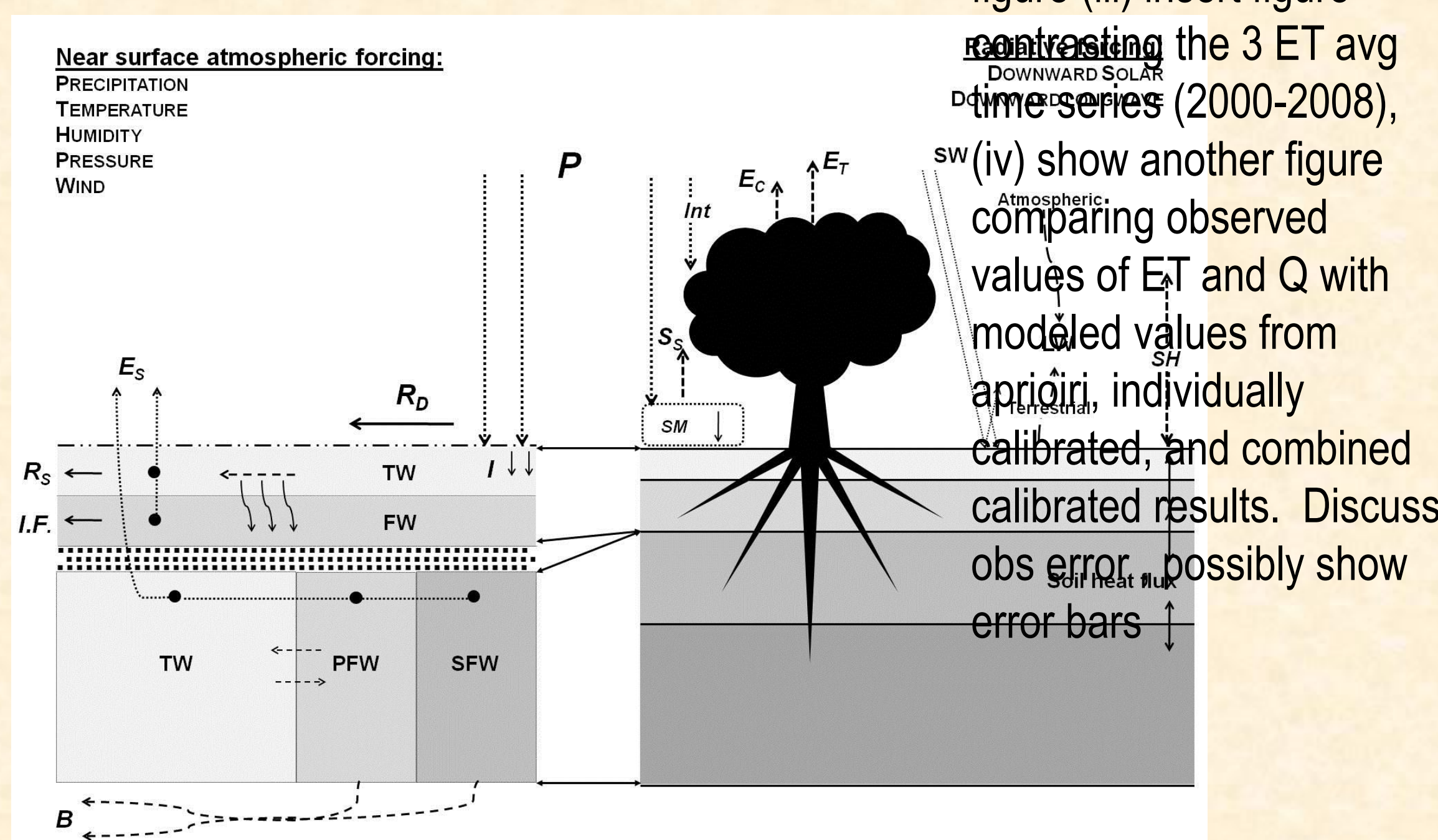


Fig. 1: Schematic of ULM, including required forcing variables, moisture and energy components. Precipitation, P , and snowmelt, SM , are partitioned into direct runoff, R_d , infiltration, and evapotranspiration. Infiltration becomes either surface runoff, R_s , or interflow, $I.F.$, in the upper zone, the remains of which can then infiltrate further into the lower zone and become baseflow, B . The double arrows represent the transfer of model structure, wherein the Sac-based soil schematic on the left is only considered for soil moisture computations (via upper and lower zone tension water, TW , and free water, FW , including primary, PFW , and secondary, SFW , storages in the larger lower zone), while the schematic on the right is used for all other model computations (including vapor transfer terms from canopy, E_c , soil, E_s , transpiration, E_r , and snow, S_s , sensible heat flux, SH , and the computation of net shortwave, SW , and longwave, LW , radiation).

Initial model evaluation

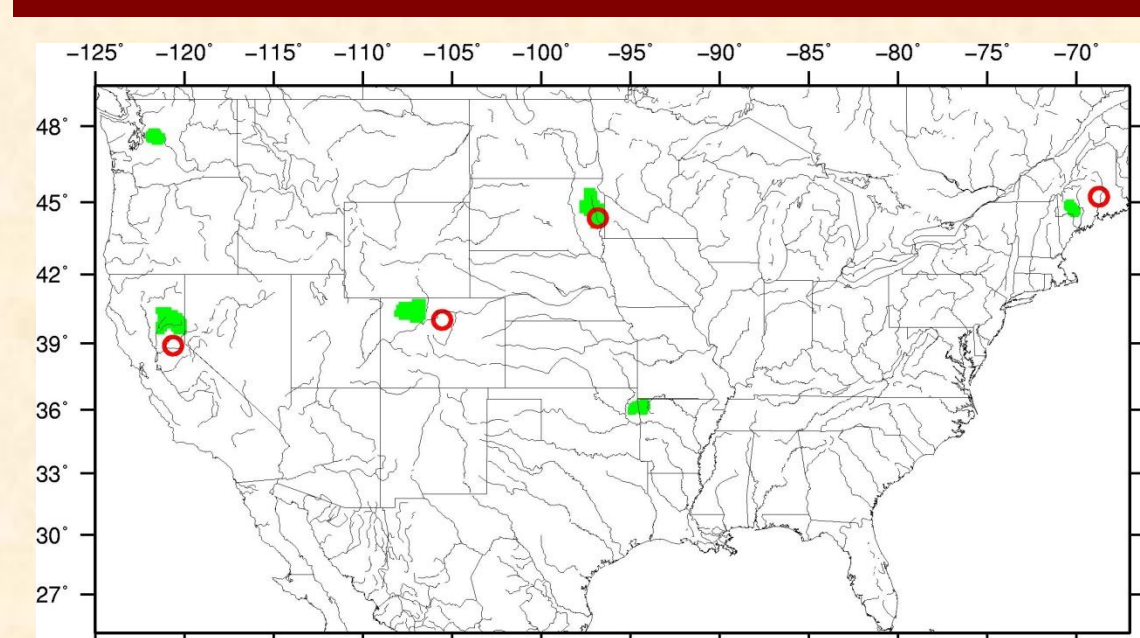


Fig. 2: Location of MOPEX study basins (green) and collocated Ameriflux flux towers (red).

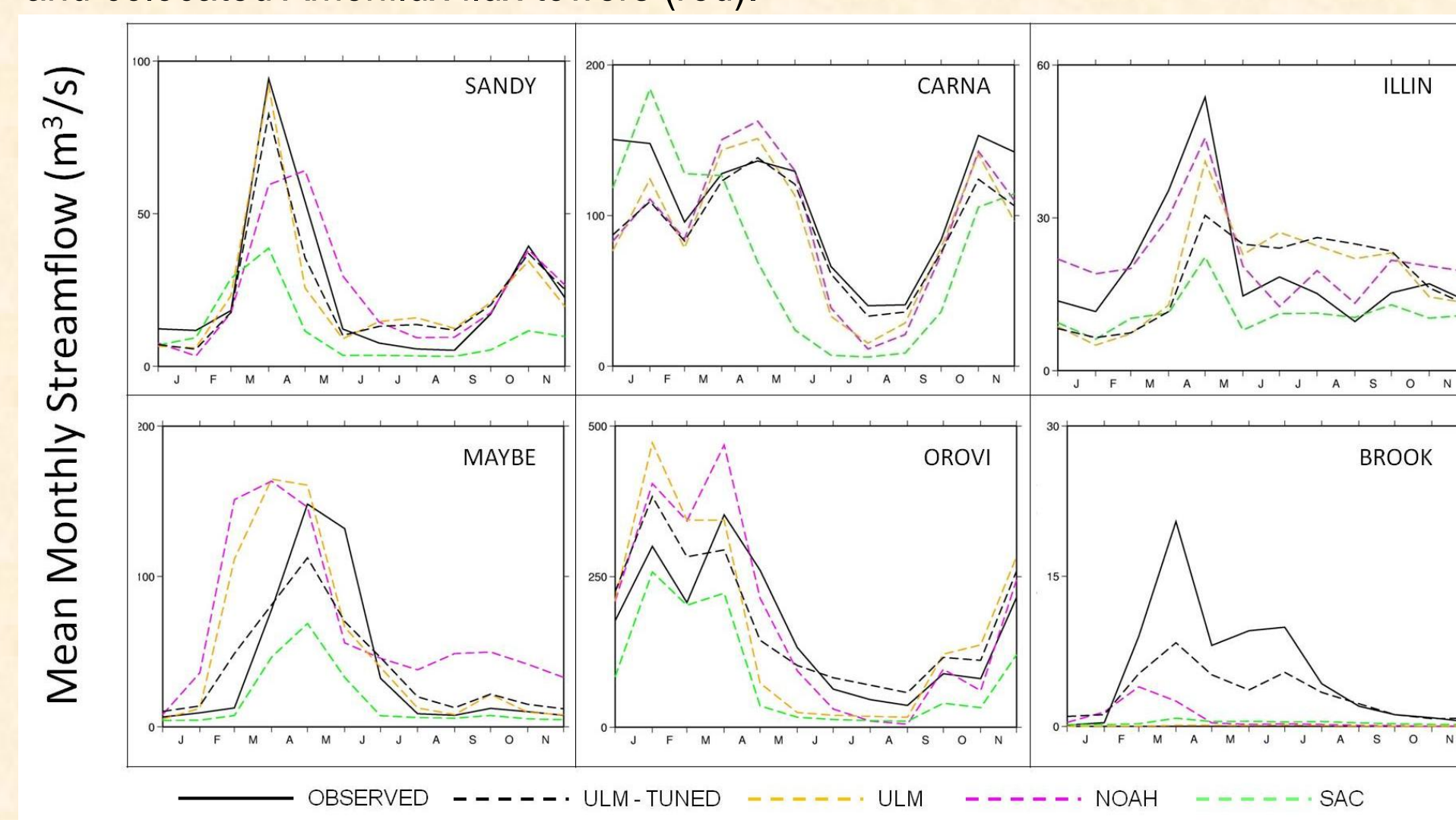


Fig. 3: Mean monthly streamflows (1960 – 1969) for ULM using apriori parameters, ULM with parameters tuned towards maximized model efficiency, Noah, Sac, and observations for the Sandy R. near Mercer, ME (SANDY), Snoqualmie R. near Carnation, WA (CARNA), Illinois R. near Tahlequah, OK (ILLIN), Yampa R. near Maybell, CO (MAYBE), Feather R. above Oroville Dam, CA (OROVI), and the Big Sioux R. near Brookings, SD (BROOK). [Flows during the evaluation period 1990-1999 were comparable to those shown above]

ULM was evaluated at for a set of river basins that span a range of hydroclimatic regimes (Figure 2). Initial testing used a priori parameters from the each parent model (Noah-NLDAS; Sac-Koren et al., 2003), followed by an assessment of ULM parameter sensitivities and limited calibration, primarily focusing on streamflow performance. Figure 3 shows that streamflow prediction improvements were most notable for less-arid basins, while parameter tunings were necessary to achieve improvements over all study basins, the majority of which were obtained through adjusting only the 3 most sensitive model soil parameters (not shown).

Partitioning of net radiation into surface heat fluxes was done at 4 locations (Figure 4). In general, ULM

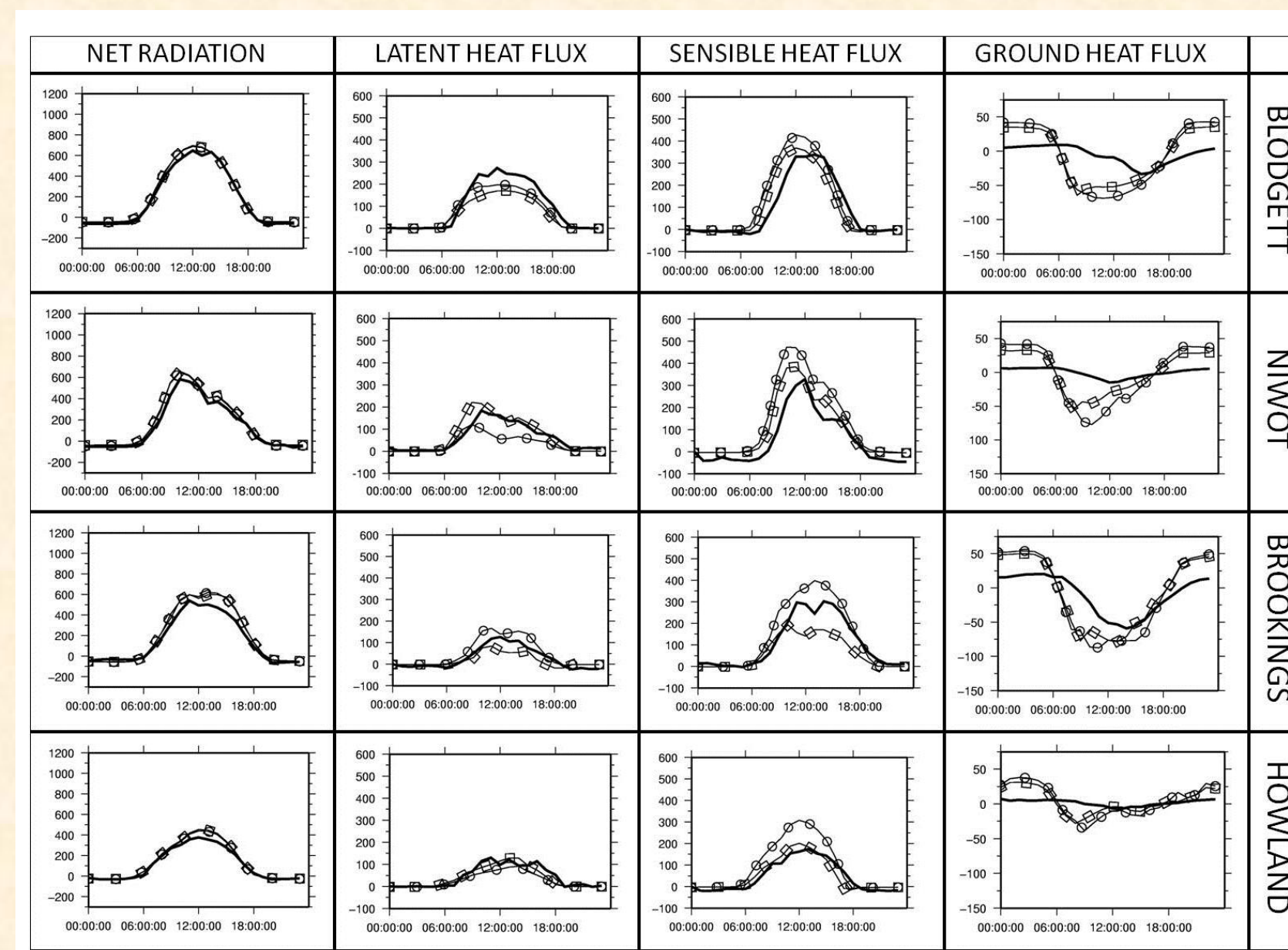


Fig. 4: Mean diurnal fluxes (W/m^2) for ULM during summer for 4 Ameriflux sites shown at 30-minute intervals over the respective year with greatest energy balance closure for Blodgett Forest, CA, Niwot Ridge, CO, Brookings, SD, and Howland Forest, ME.

performed similarly to Noah, or slightly better as compared with observations. More limited soil moisture testing was done, due to lack of quality data at these sites, where ULM was again similar to Noah, with the exception of improved performance during the soil drying phase. Attempts were made to transfer model parameters from streamflow tunings to heat flux and soil moisture simulation without a conclusive addition in model performance.

Evaluation of the terrestrial water budget with focus on ET

The focus of this experiment is to estimate areal ET at the land surface using three independent methods. First, at large scales ($\geq 100,000 km^2$) ET can be estimated through an atmospheric water balance as the residual term between precipitation, changes in precipitable water and moisture convergence in an overlying atmospheric column, as shown in Figure 5. The domain for large-scale ET estimation is shown in Figure 6 along with stream gauges by basin. Second, we consider an entirely satellite-based estimate of ET following Tang et al., 2009, that utilizes an empirical relationship between vegetative cover and surface temperature ($VI-T_s$) as shown in Figure 7. Third, ET is estimated from ULM simulation, which is the sum of resistance based estimates of soil and canopy evaporation, whilst using a Jarvis-type transpiration formulation. This final method allows for an examination of other water budget terms to assess the overall partitioning of each component in the balance. Figure 8 compares these sources. The first two methods agree on the peak magnitude of ET for western basins, although peak timing is always sooner in the first method. For basins with large disparities in the first two methods, ULM shows even larger differences, generally underestimating peak monthly ET, suggesting that parameter calibrations could be beneficial.

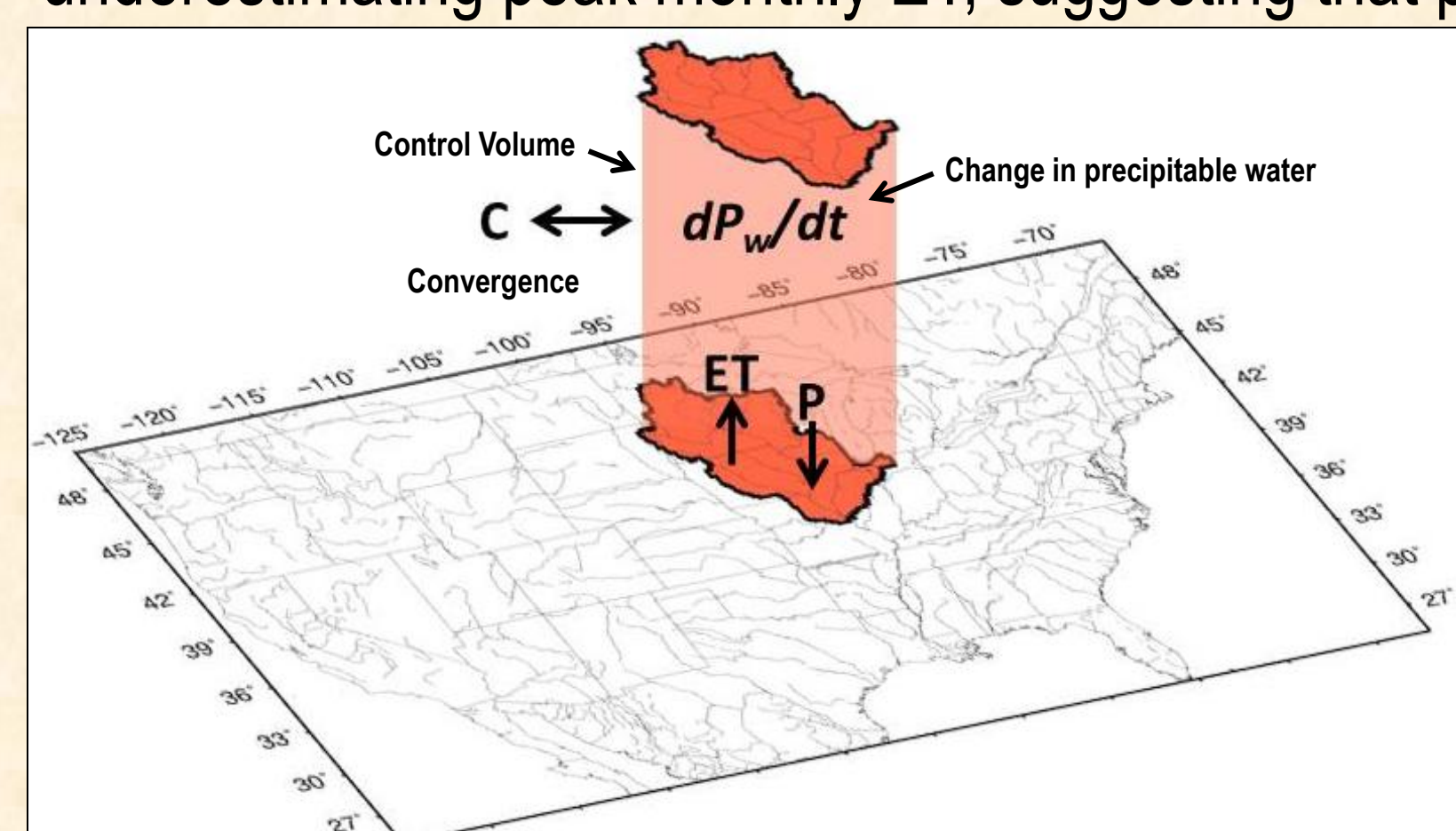


Fig. 5: Example of the Upper Mississippi river basin, schematic of the components to perform an atmospheric water balance needed to estimate ET, including atmospheric moisture convergence, C , change in precipitable water, dP_w/dt , and precipitation, P , where precipitation is from NCDG gauge data, atmospheric terms are from NARR data (Messinger et al., 2006)

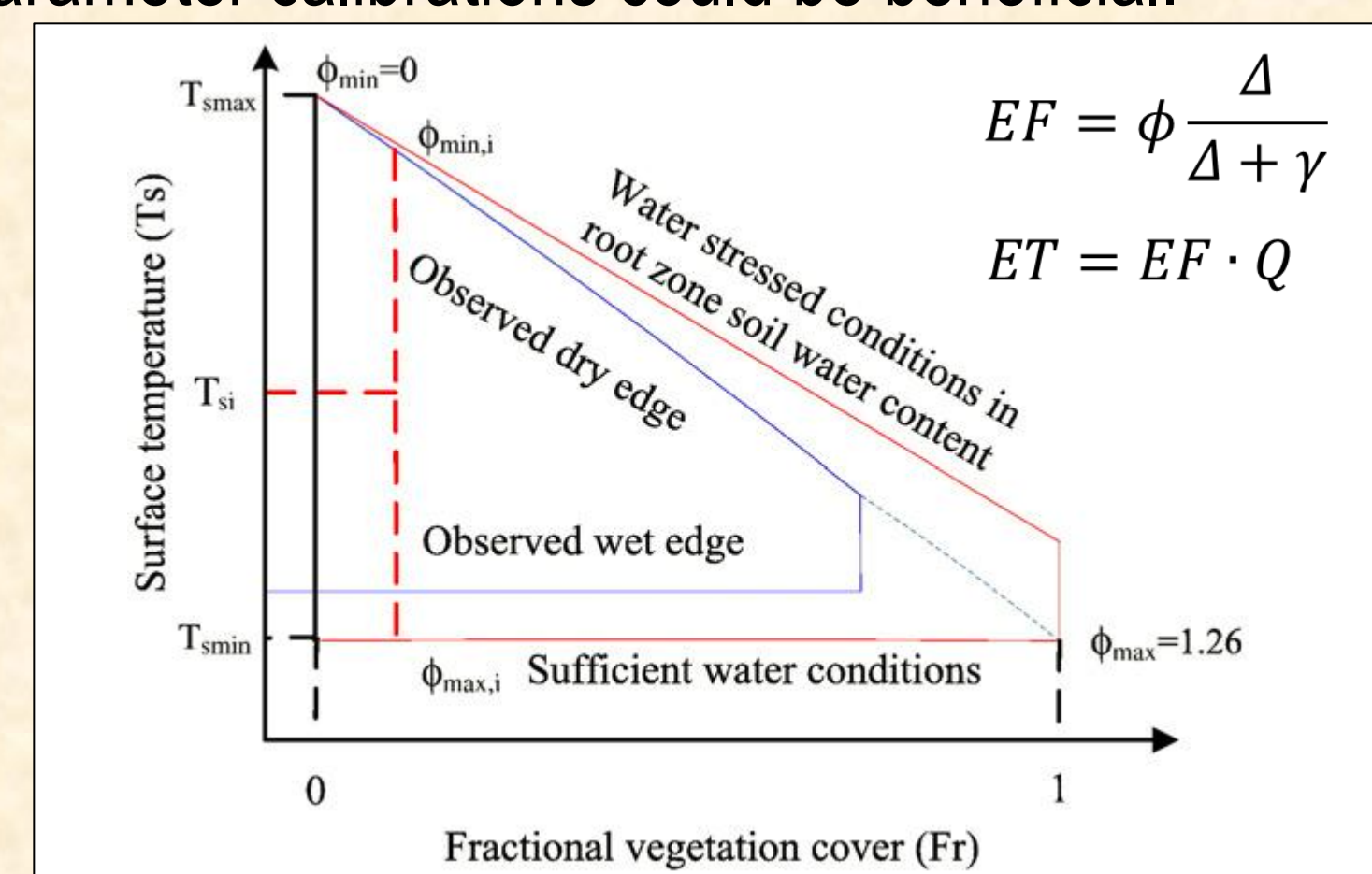


Fig. 7: Empirical relationship between surface temperature and fractional vegetation cover used (with other quantities) to compute the evaporative fraction (EF) in relation to available energy (Q) following a Priestly-Taylor analogue via slope of sat. vapor pressure vs. air pressure, Δ , and psychrometric constant, γ (from Tang et al., 2010)

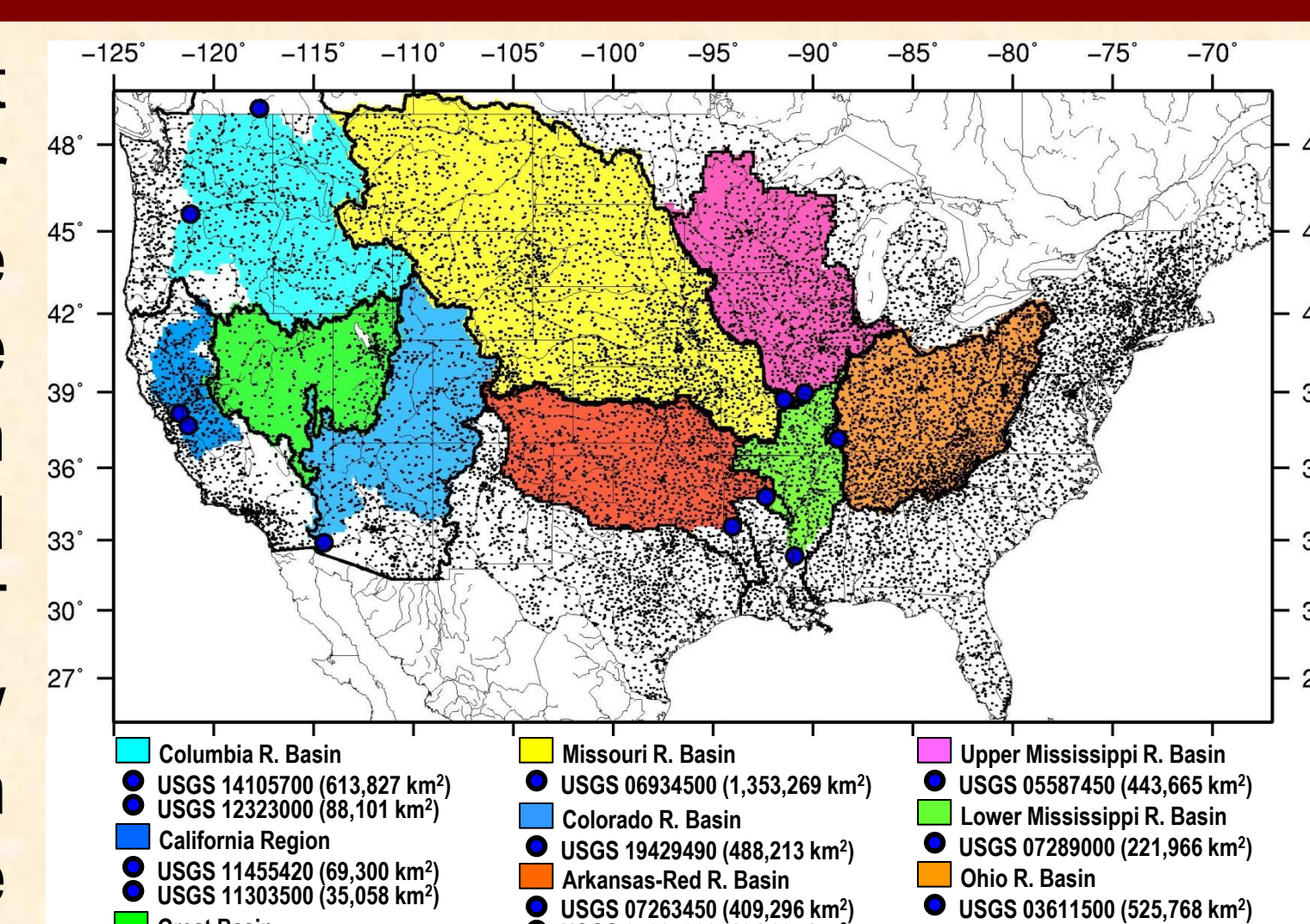


Fig. 6: Large-scale study domain, including precipitation gauges (black dots), as well as major hydrologic regions (shaded) that are defined through their drainage at stream gauges (blue circles).

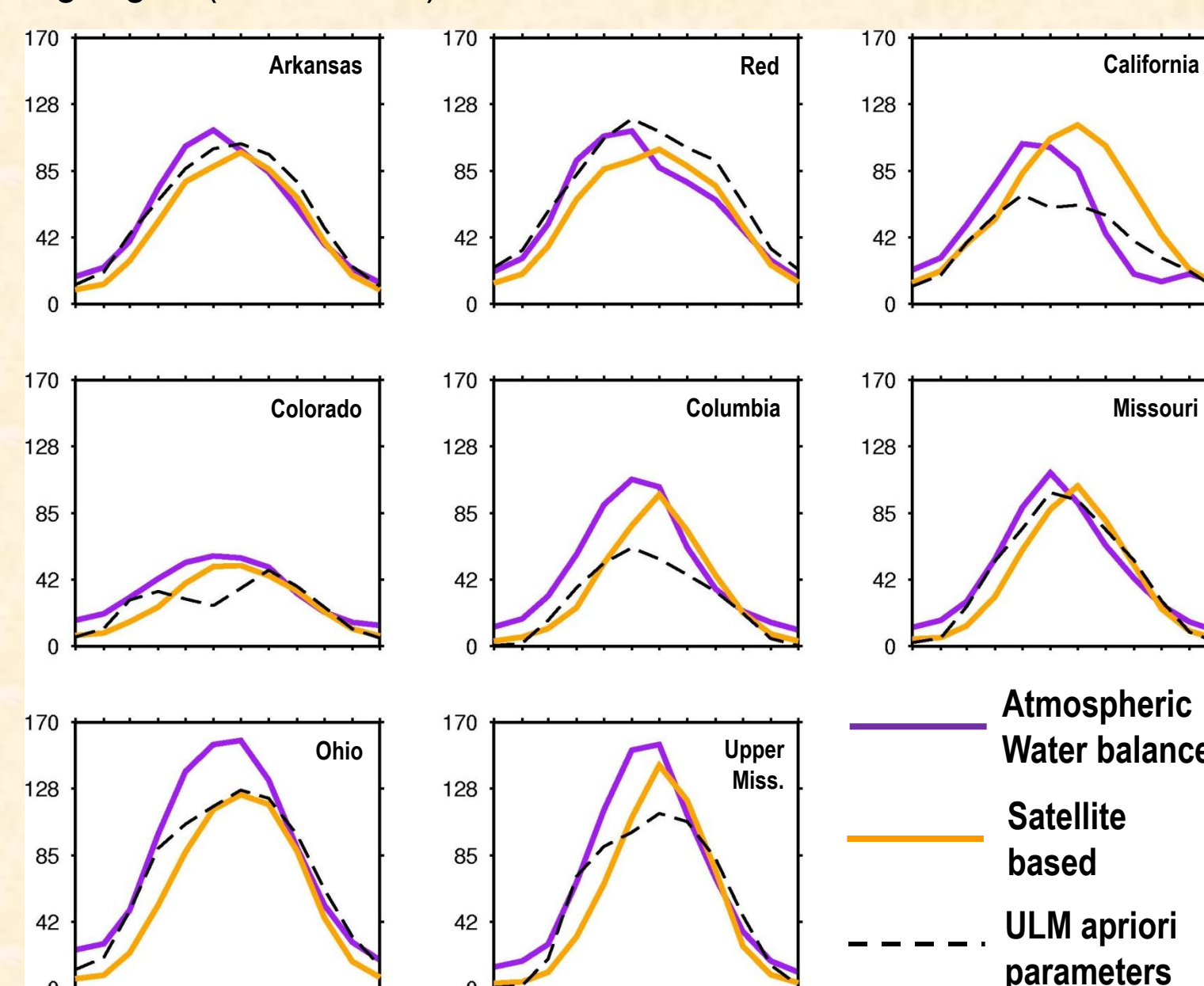


Fig. 8: Comparison of mean monthly ET (2001-2008) from two independent observation sources along with ULM.

Calibrations, stream flow and further testing

Preliminary results are for model simulations using apriori parameters only. Model residuals are shown in Figure 9. ULM generally underpredicts peak (summer) ET, reflecting a lag in peak timing. For basins where snowmelt contributes a large portion of the hydrograph, the timing and magnitude of peak ULM runoff is notably different from the gauge value, likely attributable to differences in timing of peak SWE, as well as adjustments needed in model parameters to more adequately store and transmit runoff. Figure 9 shows a CDF of annual peak flows, indicating a general over-estimation of large flood events by ULM. The domain for upcoming catchment-scale analysis is given in Figure 10.

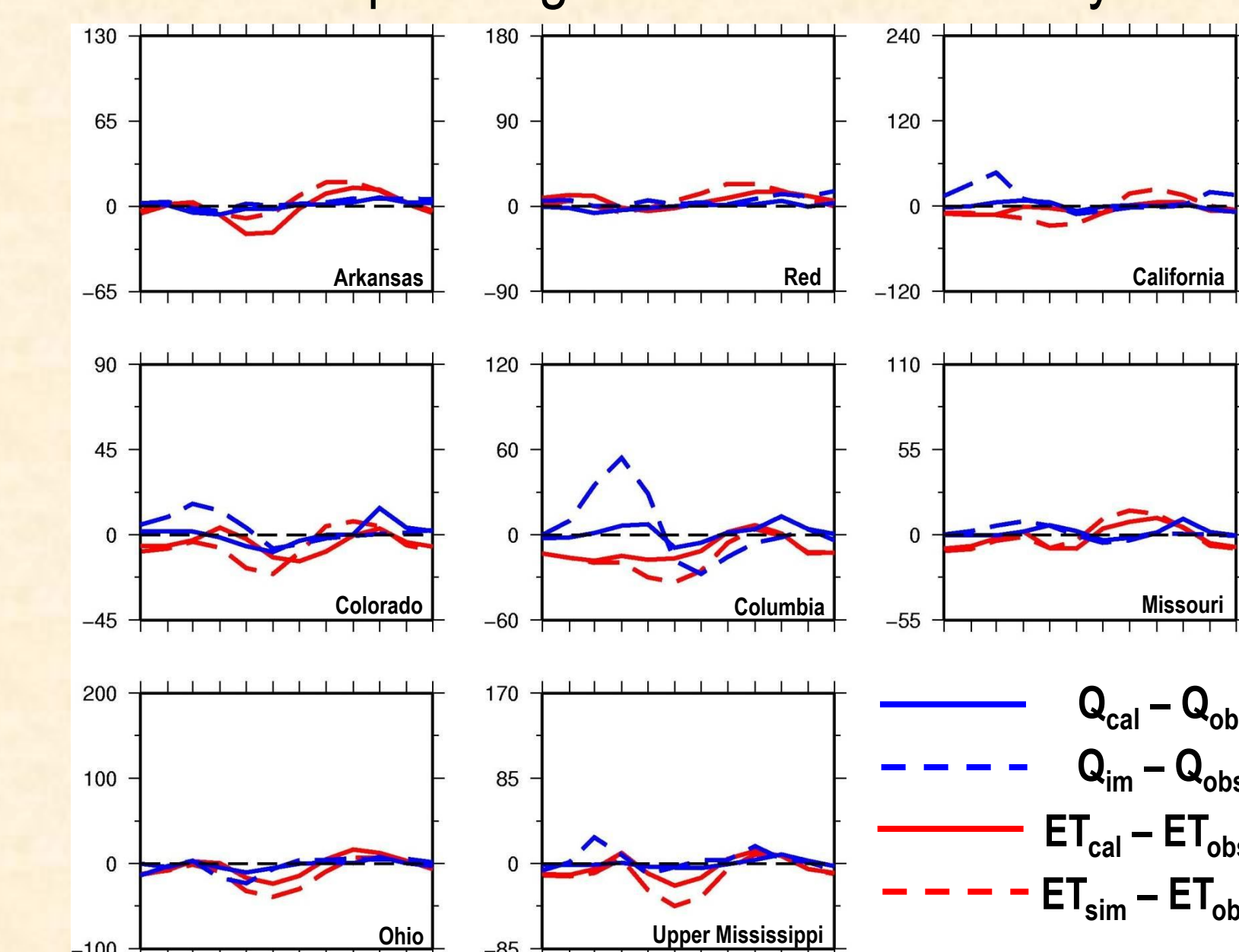


Fig. 8: (left) Mean monthly residuals between observed (obs) and simulated with apriori parameters (sim) as well as calibrated (cal) ET and streamflow 1979-2008.

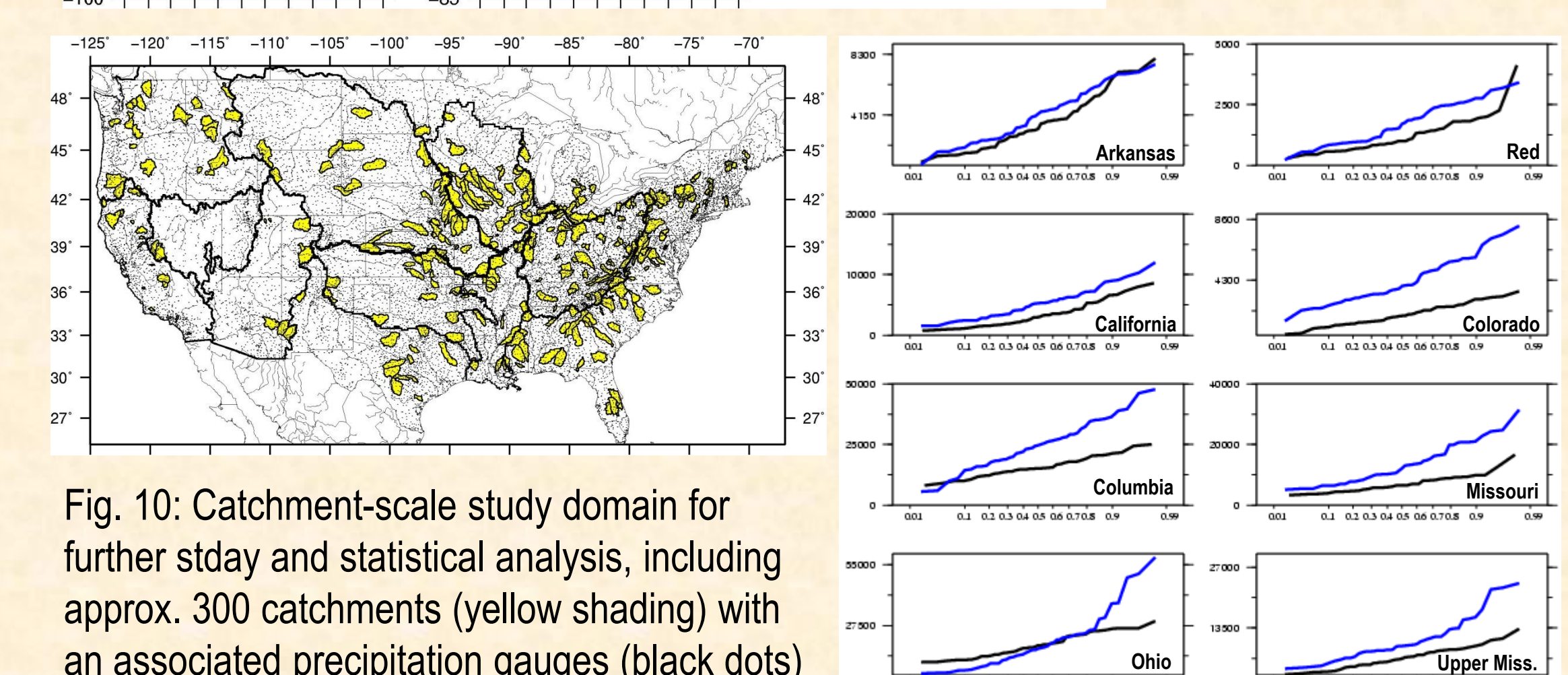


Fig. 9: (below) Cumulative distribution functions (CDF) of modeled (blue) and observed (black) annual peak flows (1979-2008).

References

Livneh, B., P.J. Restrepo, and D.P. Lettenmaier, 2010: Development of a Unified Land Model, *J. Hydrometeorol.* (submitted)
Koren V.I., M. Smith and Q. Duan, 2003: Use of a priori parameter estimates in the derivation of spatially consistent parameter sets of rainfall-runoff models. In: Q. Duan, S. Sorooshian, H. Gupta, H. Rosseau and H. Turcotte, Editors, *Calibration of Watershed Models, Water Science and Applications vol. 6*, AGU, pp. 239–254.
Koren, V.I., 2006: Parameterization of frozen ground effects: sensitivity to soil properties, in *Predictions in Ungauged Basins: Promises and Progress* (Proceedings of symposium S7 held during the Seventh IAHS Scientific Assembly at Foz do Iguaçu, Brazil, April 2005). *IAHS Publ.* 303, 125-133.
Kanamaru, H., G.D. Salvucci, and D. Entechabi, 2004: Central U.S. Atmospheric Water and Energy Budgets Adjusted for Diurnal Sampling Biases Using Top-of-Atmosphere Radiation. *J. Climate.*, 17, 2454–2465.
Tang, Q., S. Peterson, R. H. Cuenca, Y. Hagimoto, and D. P. Lettenmaier, 2009: Satellite-based near-real-time estimation of irrigated crop water consumption, *J. Geophys. Res.*, 114, D05114, doi:10.1029/2008JD010854.